

From partons to new physics at the **Large Hadron Collider**

**Global picture of QCD
and new discoveries**

Pavel Nadolsky

Michigan State University

April 30, 2008

Road map toward new discoveries at the LHC

- Re-discovery (re-learning) of the Standard Model
 - ▶ detector calibration, luminosity measurement, “standard candle” cross sections, PDF’s,...
- First observed signatures of new physics
 - ▶ new resonances, excessive event rates...
- Discrimination between new physics models based on detailed results from LHC and other experiments
 - ▶ SUSY vs. extra dimensions vs. strong dynamics vs. ...

Road map toward new discoveries at the LHC

Quite likely, these stages will be concurrent rather than consecutive; they will involve stepwise improvements in

- precise $N^x\text{LO}$ perturbative calculations+resummations
(C. Oleari's talk)
- implementation of **all** relevant pert. and nonpert. effects in the analysis of parton distributions (PDF's) and other nonperturbative functions
- Rapid inclusion of new, more sensitive, experimental data
- Resolution of new mysteries and tensions arising between theory and experiment

Tevatron Run-2: surprises in high-statistics data

- $p\bar{p} \rightarrow ZX$: significant excess in event rate at high p_T

(*DO Coll., PRL 100, 102002 (2008)*), not observed in Run-1

$$\frac{\text{data}}{\text{theory at } O(\alpha_s^2)} \sim 1.3 \text{ at } p_T \approx M_W$$

- $p\bar{p} \rightarrow ZX$: -7% (+9%) disagreement of $d\sigma/dy$ with NNLO (NLO) predictions (*CDF public note, Feb. 2008, 2.1 fb⁻¹*)

- 2σ difference between W mass measured in $W \rightarrow e\nu$ and $W \rightarrow \mu\nu$ decay modes (*CDF, PRL 99, 115801 (2007)*)

$$M_W(e\nu) = 80.477 \pm 0.062 \text{ GeV}/c^2$$

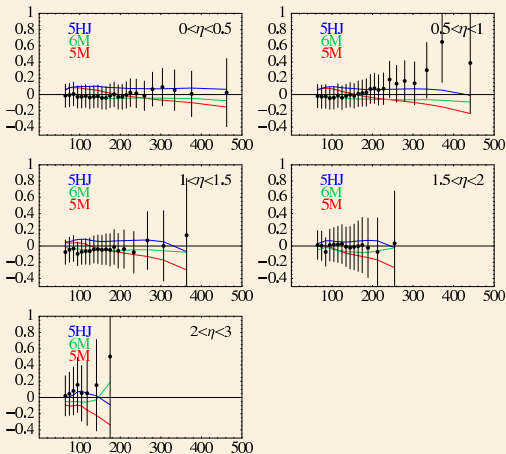
$$M_W(\mu\nu) = 80.352 \pm 0.060 \text{ GeV}/c^2$$

The probability for the combined (“single most precise”) measurement $M_W = 80.413 \pm 0.048 \text{ GeV}/c^2$ is low (7%)

- Substantial differences between the Run-1 and Run-2 inclusive jet data

See figures in C. Gerber's talk

Inclusive jet production in Tevatron Run-1

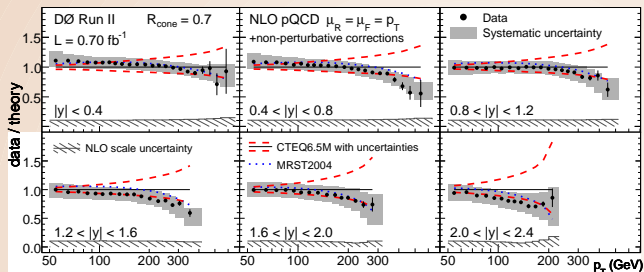


■ CDF, 1993: excess in high- E_T jet data over NLO theory based on contemporary “central-fit” PDFs (*CTEQ3M, 4M, 5M*)

■ 2001: Supported by D0 data in separate pseudorapidity regions (cf. figure)

■ Accommodated by assuming a larger gluon PDF $g(x)$ at $x \gtrsim 0.1$ (*CTEQ4HJ, 5HJ, 6xM*)

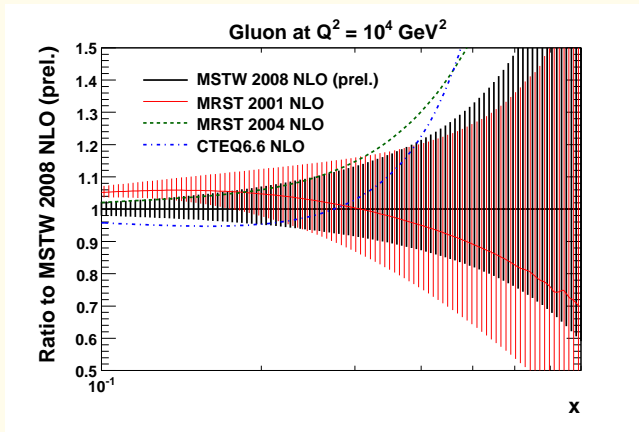
Inclusive jet production in Tevatron Run-2



*D0 Coll., arXiv:0802:2400
(700 pb⁻¹); similar tendency in
CDF results (1.13 fb⁻¹)*

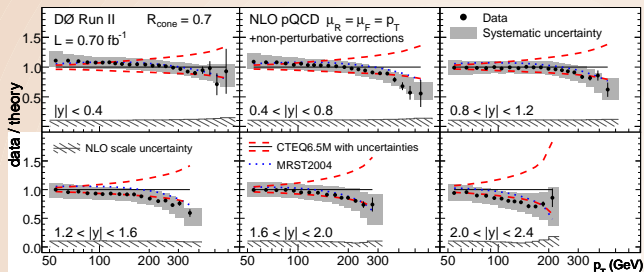
- (Almost) negligible statistical error
- MidCone/ k_T algorithm samples, corrected to parton level
- Cross sections are now smaller at high E_T !

Impact of Run II jet data on high- x gluon distribution



- Run II jet data prefer smaller gluon distribution at high x .

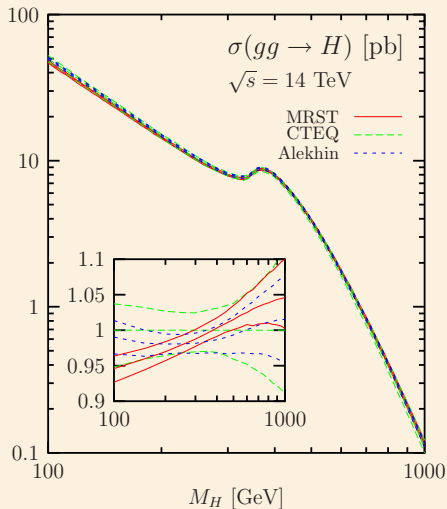
Inclusive jet production in Tevatron Run-2



DØ Coll., arXiv:0802:2400
 (700 pb^{-1}); similar tendency in
 CDF results (1.13 fb^{-1})

- Impact on the PDF's? Harder gluons disfavored?
- Agreement with Run-1 measurements?
- Experimental correlated/uncorrelated and theoretical (NLO) systematics are well-understood?
- MSTW'08 PDF's agree with those jet data sets that have larger experimental errors

Gluon PDF's and LHC predictions



In gluon scattering processes ($gg \rightarrow t\bar{t}X$, $gg \rightarrow HX$, etc.), differences due to the choice of the PDF set may exceed nominally quoted PDF uncertainties, reflecting

- choice of the data sets constraining $g(x)$ (especially whether the jet data is included)
- treatment of correlated systematic errors in jet data
- choice of running α_s , fitted $x - Q$ region of DIS data

Approximations and uncertainties in the PDF analysis

<1> Many factors determine the form of the PDF's, including

- theoretical approximations introduced in **each** fitted process
 - ▶ order of PQCD and EW contributions
 - ▶ factorization scheme for heavy flavors, values of SM parameters (α_s , α_{EM} , etc.)
 - ▶ PDF parametrization
 - ▶ treatment of nuclear effects, higher twists
- Experimental errors propagated into PDF parametrizations
- Numerical accuracy in PDF fits, computation of tabulated PDF's by end-user programs

Approximations and uncertainties in the PDF analysis

<1> Many factors determine the form of the PDF's, including

- theoretical approximations introduced in **each** fitted process
 - ▶ order of PQCD and EW contributions
 - ▶ factorization scheme for heavy flavors, values of SM parameters (α_s , α_{EM} , etc.)
 - ▶ PDF parametrization
 - ▶ treatment of nuclear effects, higher twists
- Experimental errors propagated into PDF parametrizations
- Numerical accuracy in PDF fits, computation of tabulated PDF's by end-user programs

Theoretical aspects of W , Z boson production

Targeted theoretical accuracy: 2 – 3%, needed for calibrations and benchmark tests, real-time measurement of the LHC luminosity (*Dittmar, Pauss, Zurcher; Khoze, Martin, Orava, Ryskin; Giele, Keller';...*)

Predictions for W , Z cross sections (including PDF dependence) were recently explored as a part of CTEQ6.6 PDF analysis

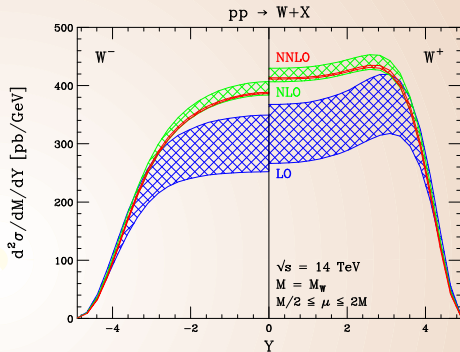
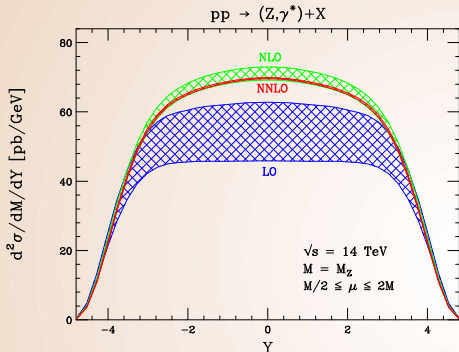
(*arXiv:0802.0007*)

- CTEQ6.6M standard set and 44 extreme eigenvector sets are available in the LHAPDF-5.4 library and at www.cteq.org
- several improvements w.r.t. CTEQ6.5 PDF's (late 2006)
- revised numerical programs with NNLO evolution; public fits still done at NLO

The MSTW group confirms our main findings

W and Z rapidity distributions at NNLO

(Anastasiou, Dixon, Melnikov, Petriello, 2003)



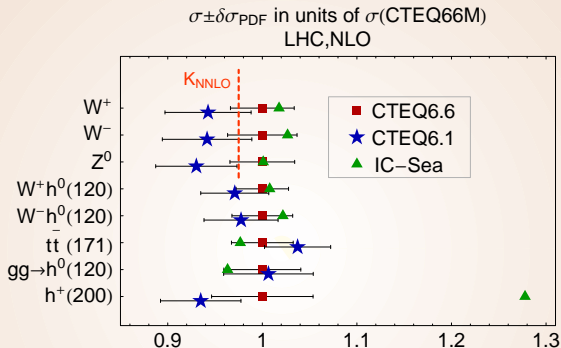
- Tiny scale dependence ($\sim 1\%$)
- For $|y| < 2$, NNLO leads to a uniform rescaling

$$\sigma_{NNLO} \approx K_{NNLO} \cdot \sigma_{NLO}; K_{NNLO}^{LHC} \approx 0.98$$

- Larger corrections at forward rapidities

LHC cross sections

General-mass CTEQ6.6, CTEQ6.6C vs. zero-mass CTEQ6.1



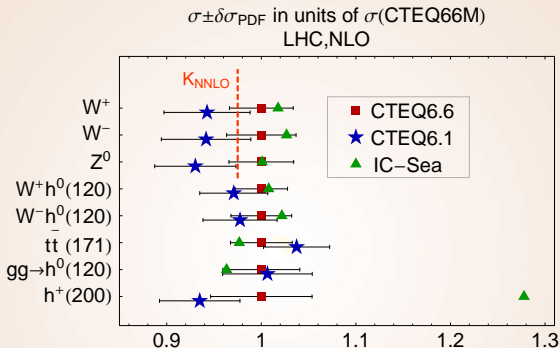
■ At the LHC, $\sigma_{W,Z}(\text{CTEQ6.6M}) \approx 1.06 \sigma_{W,Z}(\text{CTEQ6.1M})$

► reflects a 6% increase in light quark luminosities

$$\mathcal{L}_{q_i \bar{q}_j}(x_1, x_2, Q) = q_i(x_1, Q) \bar{q}_j(x_2, Q) \text{ at relevant } x \text{ and } Q$$

LHC cross sections

General-mass CTEQ6.6, CTEQ6.6C vs. zero-mass CTEQ6.1



- Such changes in $\sigma_{Z,W}$ exceed NNLO corrections or anticipated experimental error of $\sim 1\%$
- MRST'04 (MSTW'06) predictions are incompatible (compatible) with the CTEQ6.6 result

CTEQ6.5 and CTEQ6.6: advanced treatment of heavy quarks

1. full implementation of the **general-mass “SACOT- χ ” scheme**

- ▶ differences in predictions for c, b scattering ($F_2^{c,b}(x, Q^2)$, etc.), EW precision cross sections, as compared to the zero-mass CTEQ6.1

*Tung et al., JHEP 0702,
053 (2007); CTEQ6.5*

2. exploration of **free strange PDF's** and/or asymmetric strange sea

$$s_+(x) \neq r (\bar{u}(x) + \bar{d}(x)), \quad s_-(x) \neq 0,$$

where $s_{\pm}(x) \equiv s(x) \pm \bar{s}(x)$

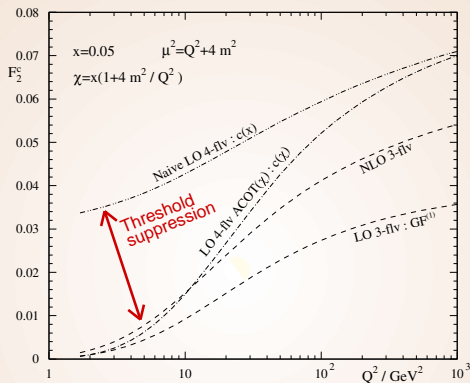
*Lai et al., JHEP 0704,
089 (2007); CTEQ6.5S*

3. PDF's with **nonperturbative charm**

- ▶ $c(x, \mu_0 = m_c) \neq 0$ due to low-energy charm excitations (as opposed to $g \rightarrow c\bar{c}$ radiative production)

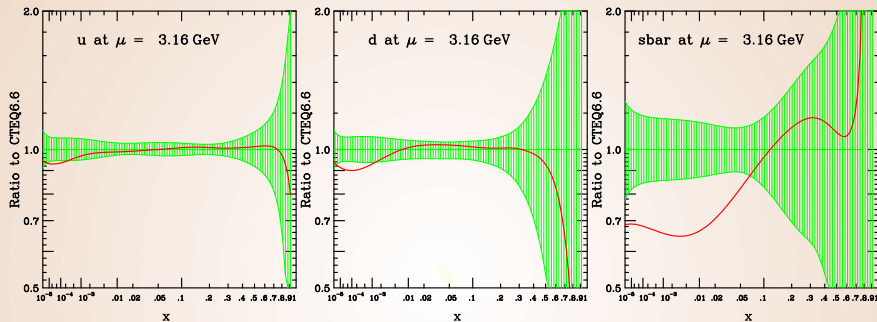
*Pumplin et al., PRD 75,
054029 (2007);
CTEQ6.5C*

General-mass (ACOT- χ) factorization scheme



- Charm Wilson coefficient function is suppressed at $Q \rightarrow m_c$
- To keep agreement with DIS F_2 data, u , d , \bar{u} , \bar{d} PDF's are enhanced at small x , as compared to the zero-mass (ZM-VFN) scheme

CTEQ6.6 PDF's



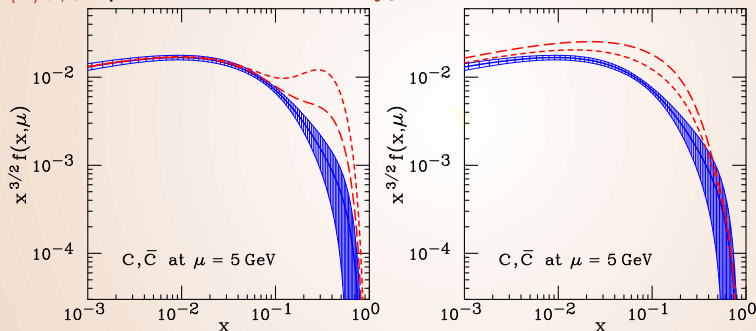
dashes: CTEQ6.1M (zero-mass scheme)

- CTEQ6.6 u, d are above CTEQ6.1 at $x \lesssim 10^{-2}$
 - ▶ The result of suppressed charm contribution to $F_2(x, Q)$ at HERA in the GM-VFN scheme
- very different strange PDF's

Special PDF's with nonperturbative charm

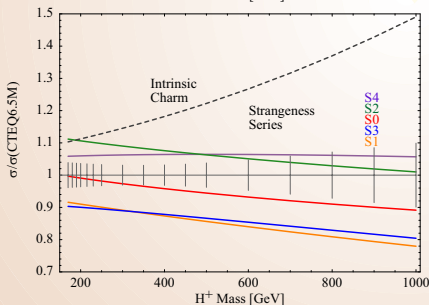
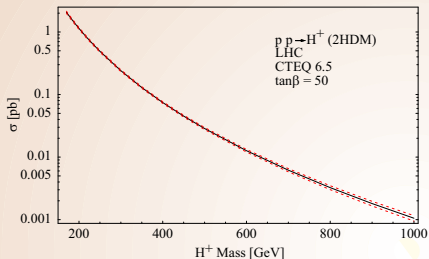
(Pumplin et al., 2007; updated in CTEQ6.6C)

Three models responsible for intrinsic charm generation (light-cone, meson-cloud, and phenomenological sea-like), with $\langle x \rangle_{c+\bar{c}}$ up to 3.5% at scale Q_0



The enhancement in $c(x, Q)$ persists at all practical Q , can be observed at the Tevatron and LHC

$c\bar{s} + c\bar{b} \rightarrow H^+$ in 2-Higgs doublet model at the LHC



CTEQ6.6M uncertainty band covers most of the CTEQ6.5 uncertainty due to strangeness

“Maximum-strength” sea-like IC leads to large enhancement \Rightarrow new measurements ($p\bar{p} \rightarrow ZcX?$) are needed to constrain it!

Approximations and uncertainties in the PDF analysis

<1> Many factors determine the form of the PDF's, including

- theoretical approximations introduced in **each** fitted process
 - ▶ order of PQCD and EW contributions
 - ▶ factorization scheme for heavy flavors, values of SM parameters (α_s , α_{EM} , etc.)
 - ▶ PDF parametrization
 - ▶ treatment of nuclear effects, higher twists
- Experimental errors propagated into PDF parametrizations
- Numerical accuracy in PDF fits, computation of tabulated PDF's by end-user programs

Experimental PDF errors: which measurements can reduce them?

Knowing what to measure and how to measure it makes a complicated world much less so.

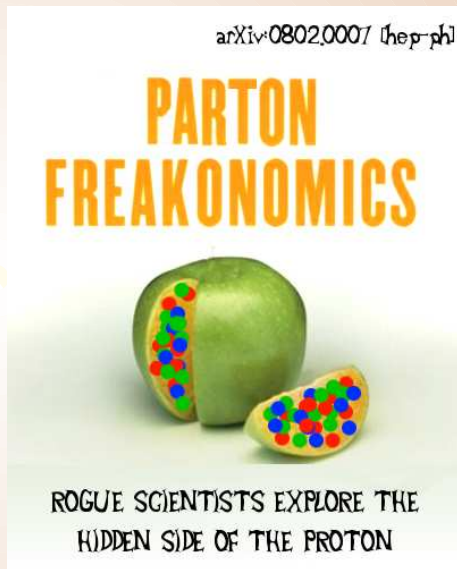
The conventional wisdom is often wrong.

S. D. Levitt, S. J. Dubner, Freakonomics

PDF dependence of collider processes

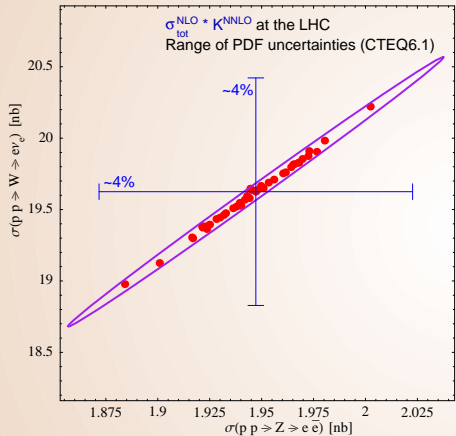
- Naive views about the PDF dependence tend to be misleading
- Substantial PDF-induced (anti)correlations exist between large classes of collider cross sections
- These correlations can be explored as a part of the global analysis

⇒ implications for parton and collider luminosity measurements, determination of new physics parameters

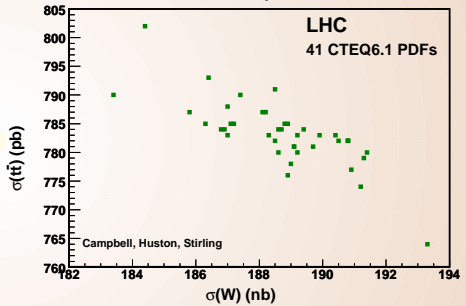


PDF-induced correlations in $W, Z, t\bar{t}$ production

$W - Z$: correlated dependence



$W - t\bar{t}$ (or $Z - t\bar{t}$):
anti-correlated dependence



The PDF dependence of a cross section ratio σ_1/σ_2 is reduced (enhanced) if σ_1 and σ_2 are correlated (anticorrelated)

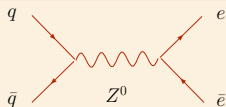
Z production at the LHC

Choose all that apply and select the x range

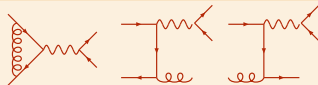
The PDF uncertainty in σ_Z is mostly due to...

1. u, d, \bar{u}, \bar{d} PDF's
at $x < 10^{-2}$ ($x > 10^{-2}$)
2. gluon PDF
at $x < 10^{-2}$ ($x > 10^{-2}$)
3. s, c, b PDF's
at $x < 10^{-2}$ ($x > 10^{-2}$)

Leading order



Next-to-leading order

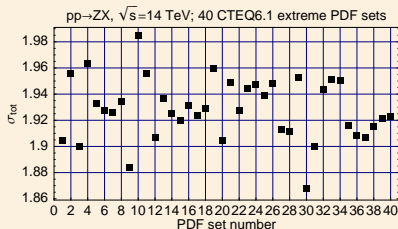


An inefficient application of the error analysis

☺ Compute σ_Z for 40 (now 44) extreme PDF eigensets

☺ Find eigenparameter(s) producing largest variation(s), such as #9, 10, 30

☹ It is not obvious how to relate abstract eigenparameters to physical PDF's $u(x)$, $d(x)$, etc.



Correlation analysis for collider observables

(J. Pumplin et al., PRD 65, 014013 (2002); P.N. and Z. Sullivan, hep-ph/0110378)

A technique based on the Hessian method to relate the PDF uncertainty in physical cross sections to PDF's of specific flavors at known (x, μ)

For $2N$ PDF eigensets and two cross sections X and Y :

$$\Delta X = \frac{1}{2} \sqrt{\sum_{i=1}^N \left(X_i^{(+)} - X_i^{(-)} \right)^2}$$

$$\cos \varphi = \frac{1}{4\Delta X \Delta Y} \sum_{i=1}^N \left(X_i^{(+)} - X_i^{(-)} \right) \left(Y_i^{(+)} - Y_i^{(-)} \right)$$

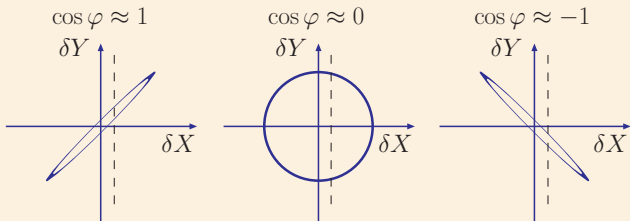
$X_i^{(\pm)}$ are maximal (minimal) values of X_i tolerated along the i -th PDF eigenvector direction; $N = 22$ for the CTEQ6.6 set

Correlation angle φ

Determines the parametric form of the $X - Y$ correlation ellipse

$$X = X_0 + \Delta X \cos \theta$$

$$Y = Y_0 + \Delta Y \cos(\theta + \varphi)$$



X_0, Y_0 : best-fit values

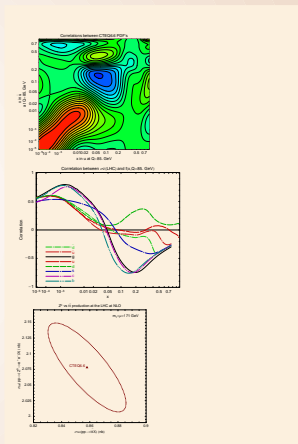
$\Delta X, \Delta Y$: PDF errors

cos $\varphi \approx \pm 1$: Measurement of X imposes tight constraints on Y
cos $\varphi \approx 0$: Measurement of X imposes loose constraints on Y

Types of correlations

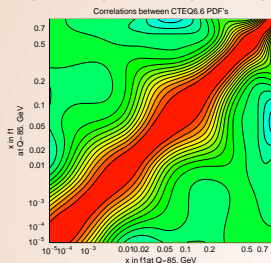
X and Y can be

- two PDFs $f_1(x_1, Q_1)$ and $f_2(x_2, Q_2)$ (plotted as $\cos \varphi$ vs x_1 & x_2)
- a physical cross section σ and PDF $f(x, Q)$ (plotted as $\cos \varphi$ vs x)
- two cross sections σ_1 and σ_2

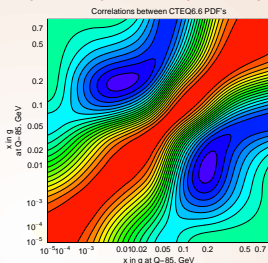


Correlations between $f(x_1, Q)$ and $f(x_2, Q)$ at $Q = 85$ GeV

$u(x_1, Q)$ vs. $u(x_2, Q)$



$g(x_1, Q)$ vs. $g(x_2, Q)$

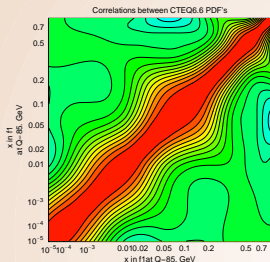


■ Momentum sum rule (affects $g(x, Q)$):

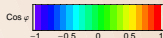
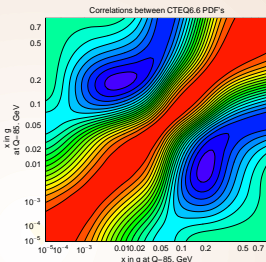
$$\int_0^1 x g(x) dx + \sum_{i=1}^{N_f} \int_0^1 x [q_i(x) + \bar{q}_i(x)] dx = 1$$

Correlations between $f(x_1, Q)$ and $f(x_2, Q)$ at $Q = 85 \text{ GeV}$

$u(x_1, Q)$ VS. $u(x_2, Q)$

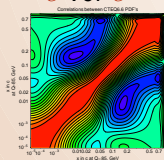


$g(x_1, Q)$ VS. $g(x_2, Q)$

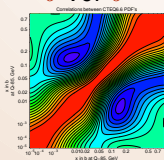


Correlation patterns look similar for g, c, b PDF's
(no intrinsic charm here!)

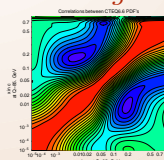
c VS. c



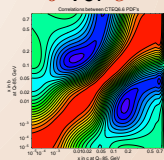
b VS. b



c VS. g



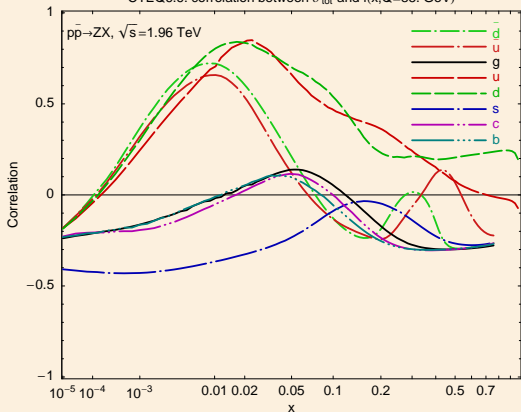
b VS. c



Correlations $\cos \varphi$ between W, Z cross sections and PDF's

Tevatron Run-2

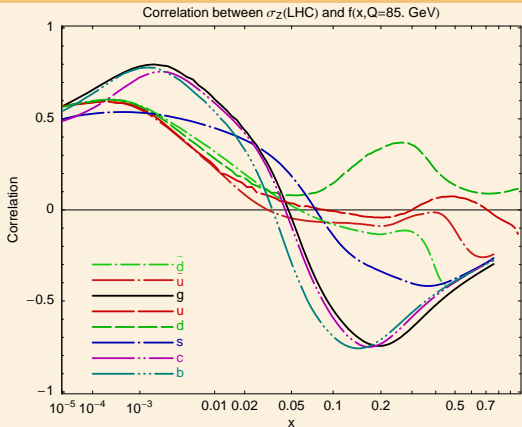
CTEQ6.6: correlation between σ_{tot} and $f(x, Q=85. \text{ GeV})$



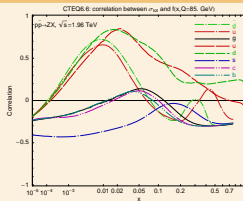
Similar correlations for W production

Correlations $\cos \varphi$ between W, Z cross sections and PDF's

LHC



Tevatron Run-2



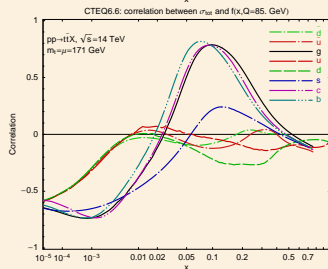
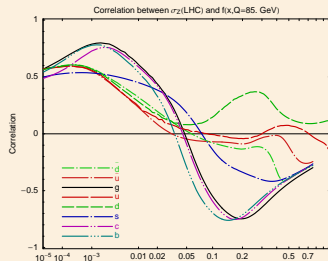
Similar correlations for W production

Correlations of Z and $t\bar{t}$ cross sections with PDF's

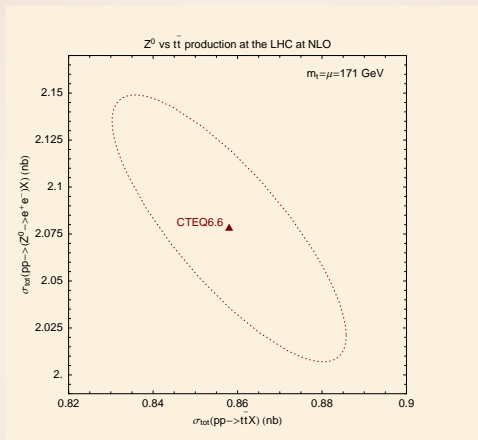
LHC Z , W cross sections are strongly correlated with $g(x)$, $c(x)$, $b(x)$ at $x \sim 0.005$

\therefore they are strongly anticorrelated with processes sensitive to $g(x)$ at $x \sim 0.1$

($t\bar{t}$, $gg \rightarrow H$ for $M_H > 300$ GeV)

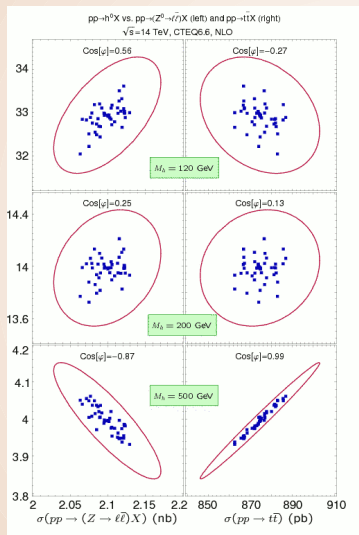


$t\bar{t}$ vs Z cross sections at the LHC



Measurements of $\sigma_{t\bar{t}}$ and σ_Z probe the same (gluon) PDF degrees of freedom at different x values

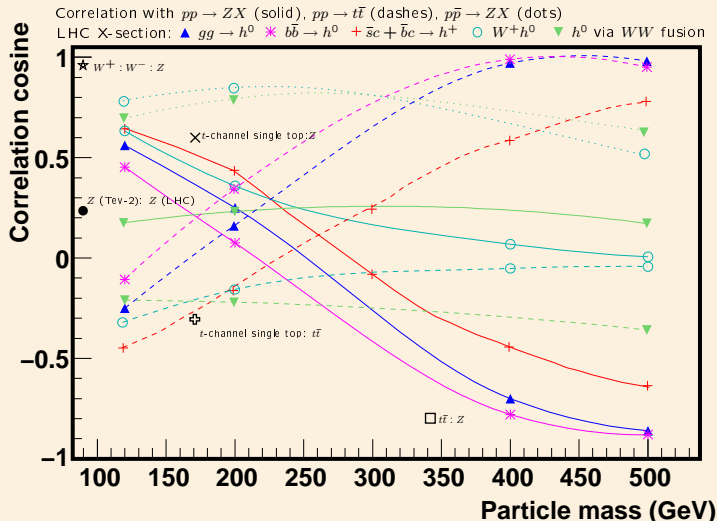
Correlations between $\sigma(gg \rightarrow H^0)$, σ_Z , $\sigma_{t\bar{t}}$



As M_H increases:

- $\cos \varphi(\sigma_H, \sigma_Z)$ decreases
- $\cos \varphi(\sigma_H, \sigma_{t\bar{t}})$ increases

$\cos \varphi$ for various NLO Higgs production cross sections in SM and MSSM



$t\bar{t}$ production as a standard candle process

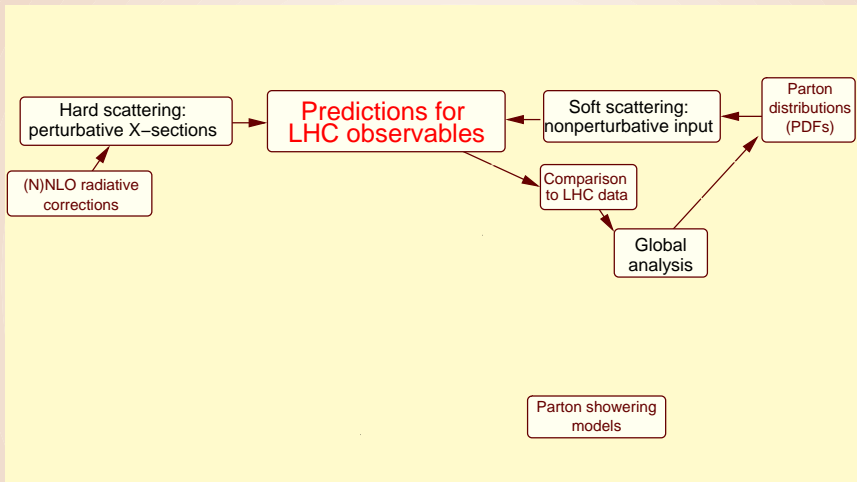
Uncertainties in $\sigma_{t\bar{t}}$ for $m_t = 171$ GeV

Type	Current	Projected	Assumptions
Scale dependence	11% (NLO)	$\sim 3 - 5\%$? (NNLO+resum.)	$m_t/2 \leq \mu \leq 2m_t$
PDF dependence	2%	1%?	1σ c.l.
m_t dependence	5% $\delta m_t = 2$ GeV	$< 3\%$ $\delta m_t = 1$ GeV	
Total (theory)	12%	$\sim 5\%$	
Experiment	8% (CDF)	5%?	

■ Measurements of $\sigma_{t\bar{t}}$ with accuracy $\sim 5\%$ may be within reach; useful for monitoring of \mathcal{L}_{LHC} in the first years, normalization of cross sections sensitive to large- x glue scattering, as well as for new physics searches (reviewed by T. Han in arXiv:0804.3178)

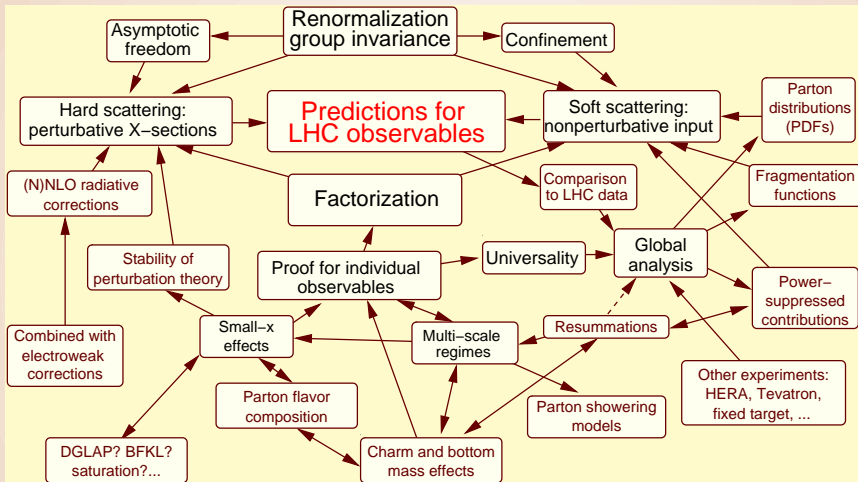
Updated theory estimates in Cacciari et al., arXiv:0804.2800; Moch, Uwer, arXiv:0804.1476

Global connections in QCD



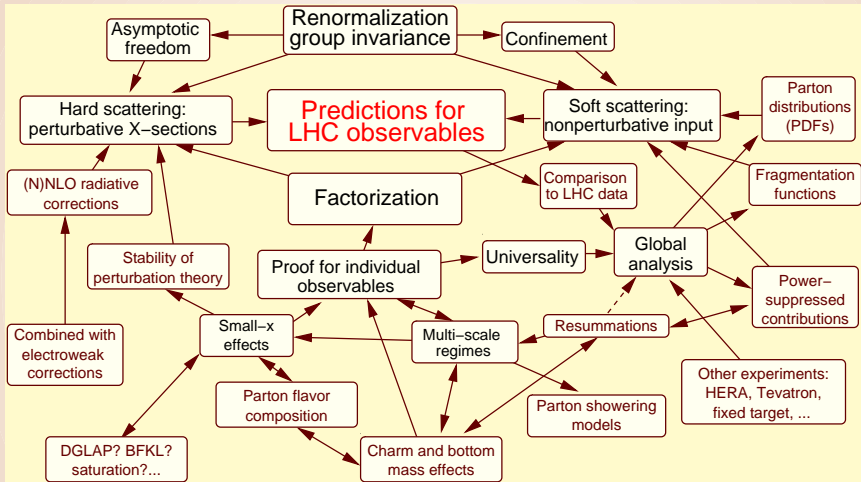
A relevant, yet incomplete, picture

Global connections in QCD



Global interconnections can be as important as (N)NLO perturbative contributions; are different at the LHC and Tevatron

Global connections in QCD

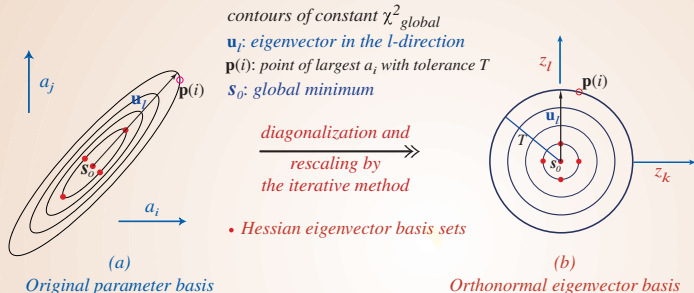


Exploration of all vastness of global QCD interconnections will greatly enrich and empower the LHC discovery program

Backup slides

Tolerance hypersphere in the PDF space

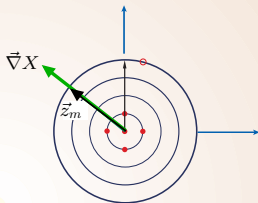
2-dim (i,j) rendition of N-dim (22) PDF parameter space



A hyperellipse $\Delta\chi^2 \leq T^2$ in space of N physical PDF parameters $\{a_i\}$ is mapped onto a hypersphere of radius T in space of N orthonormal PDF parameters $\{z_i\}$

Tolerance hypersphere in the PDF space

2-dim (i,j) rendition of N-dim (22) PDF parameter space



(b)

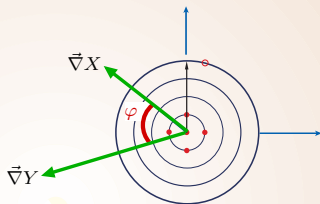
Orthonormal eigenvector basis

PDF error for a physical observable X is given by

$$\Delta X = \vec{\nabla} X \cdot \vec{z}_m = \left| \vec{\nabla} X \right| = \frac{1}{2} \sqrt{\sum_{i=1}^N \left(X_i^{(+)} - X_i^{(-)} \right)^2}$$

Tolerance hypersphere in the PDF space

2-dim (i,j) rendition of N-dim (22) PDF parameter space



(b)

Orthonormal eigenvector basis

Correlation cosine for observables X and Y :

$$\cos \varphi = \frac{\vec{\nabla}X \cdot \vec{\nabla}Y}{\Delta X \Delta Y} = \frac{1}{4\Delta X \Delta Y} \sum_{i=1}^N \left(X_i^{(+)} - X_i^{(-)} \right) \left(Y_i^{(+)} - Y_i^{(-)} \right)$$

$Z, W, t\bar{t}$ cross sections and correlations

Table: Total cross sections σ , PDF-induced errors $\Delta\sigma$, and correlation cosines $\cos\varphi$ for Z^0 , W^\pm , and $t\bar{t}$ production at the Tevatron Run-2 (TeV2) and LHC, computed with CTEQ6.6 PDFs.

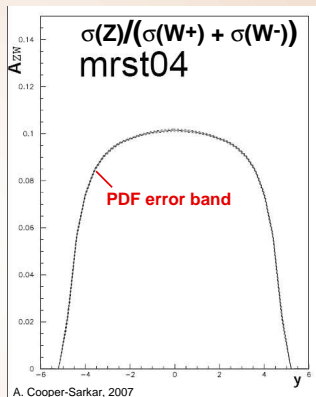
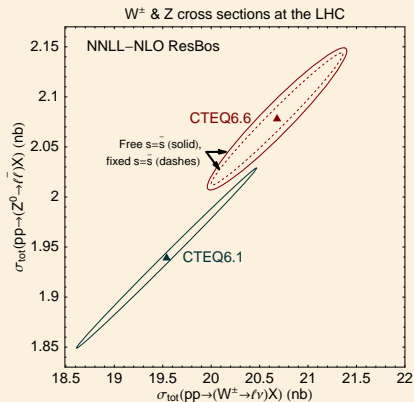
\sqrt{s} (TeV)	Scattering process	$\sigma, \Delta\sigma$ (pb)	Correlation $\cos\varphi$ with			
			Z^0 (TeV2)	W^\pm (TeV2)	Z^0 (LHC)	W^\pm (LHC)
1.96	$p\bar{p} \rightarrow (Z^0 \rightarrow \ell^+\ell^-)X$	241(8)	1	0.987	0.23	0.33
	$p\bar{p} \rightarrow (W^\pm \rightarrow \ell\nu_\ell)X$	2560(40)	0.987	1	0.27	0.37
	$p\bar{p} \rightarrow t\bar{t}X$	7.2(5)	-0.03	-0.09	-0.52	-0.52
14	$pp \rightarrow (Z^0 \rightarrow \ell^+\ell^-)X$	2080(70)	0.23	0.27	1	0.956
	$pp \rightarrow (W^\pm \rightarrow \ell\nu)X$	20880(740)	0.33	0.37	0.956	1
	$pp \rightarrow (W^+ \rightarrow \ell^+\nu_\ell)X$	12070(410)	0.32	0.36	0.928	0.988
	$pp \rightarrow (W^- \rightarrow \ell^-\bar{\nu}_\ell)X$	8810(330)	0.33	0.38	0.960	0.981
	$pp \rightarrow t\bar{t}X$	860(30)	-0.14	-0.13	-0.80	-0.74

Correlations with single-top cross sections

Table: Correlation cosines $\cos \varphi$ between single-top, W , Z , and $t\bar{t}$ cross sections at the Tevatron Run-2 (TeV2) and LHC, computed with CTEQ6.6 PDFs.

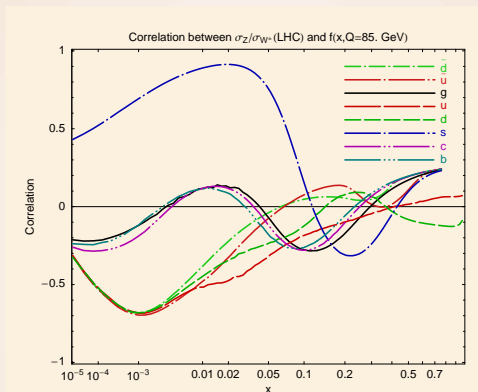
Single-top production channel	Correlation $\cos \varphi$ with					
	Z^0 (TeV2)	W^\pm (TeV2)	$t\bar{t}$ (TeV2)	Z^0 (LHC)	W^\pm (LHC)	$t\bar{t}$ (LHC)
t -channel (TeV2)	-0.18	-0.22	0.81	-0.82	-0.79	0.56
t -channel (LHC)	0.09	0.14	-0.64	0.56	0.53	-0.42
s -channel (TeV2)	0.83	0.79	0.18	0.22	0.27	-0.3
s -channel (LHC)	0.81	0.85	-0.42	0.6	0.68	-0.33

Correlations and ratio of W and Z cross sections



Radiative contributions, PDF dependence have similar structure in W , Z , and alike cross sections; cancel well in Xsection ratios

σ_Z/σ_W at the LHC



The remaining PDF uncertainty in σ_Z/σ_W is mostly driven by $s(x)$; increases by a factor of 3 compared to CTEQ6.1 as a result of free strangeness in CTEQ6.6

Tevatron Run-2: precise tests of SM physics

■ Measurements constraining the nucleon structure (PDF's)

- ▶ W boson charge asymmetry
- ▶ $d\sigma/dy$ for $p\bar{p} \xrightarrow{\gamma^*, Z} \ell^+\ell^- X$ ($\ell = e, \nu$)
- ▶ $p\bar{p} \rightarrow \text{jet} + X$ cross sections
- ▶ Z -boson $d\sigma/dp_T$

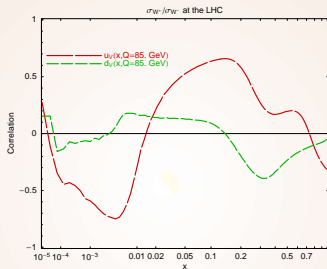
■ Measurements affected by PDF uncertainties

- ▶ collider luminosity
- ▶ $M_W, \Gamma_W, A_{FB}(p\bar{p} \rightarrow ZX), m_t, \sigma(p\bar{p} \rightarrow t\bar{t}X)$, single-top, ...

Combined with HERA-2, fixed-target data, Run-2 results bring the PDF's to a qualitatively new level of understanding

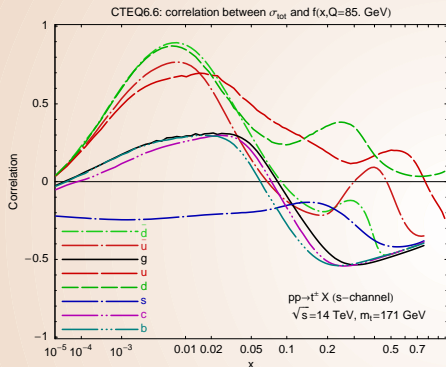
Talks by C. Gerber, J. Zhu; CDF and D0 web pages

$$\sigma(W^+)/\sigma(W^-)$$

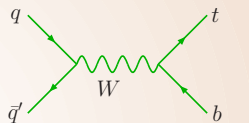


$$\sigma(W^+)/\sigma(W^-) = 1.36 + 0.016 \text{ (CTEQ6.6)}, 1.36 \text{ (MSTW'06NNLO)}, 1.35 \text{ (MRST'04NLO)}$$

An example of a small correlation with the gluon



Single-top production (NLO)



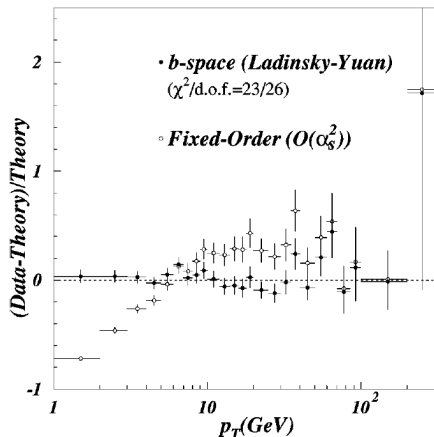
- typical $x \sim 0.01$
- mostly correlated with u, d PDF's

PDF uncertainties in W, Z total cross sections are irrelevant for some quark scattering processes (single-top, Z' , ...)

$d\sigma/dp_T$ in $p\bar{p} \rightarrow (Z \rightarrow \ell^+\ell^-)X$

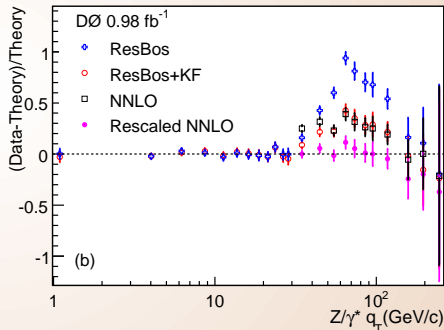
Tevatron Run-1

(D0 Coll., PRD D61, 032004 (1999))



Tevatron Run-2

(D0 Coll., PRL 100, 1020002 (2008))



$d\sigma/dy$ in $p\bar{p} \rightarrow \ell^+\ell^-X$ from CDF (2.1 fb^{-1})

